Journal of Materials Processing Tech. 255 (2018) 477–487

Contents lists available at ScienceDirect

Journal of Materials Processing Tech.

journal homepage: www.elsevier.com/locate/jmatprotec

A comparative study of microstructure and tensile properties of Ti_2AlNb joints prepared by laser welding and laser-additive welding with the addition of filler powder

Zhenglong Lei*, Kezhao Zhang, Heng Zhou, Longchang Ni, Yanbin Chen

State Key Laboratory of Advanced Welding and Joining, Harbin Institute of Technology, 150001, China

ARTICLE INFO

Keywords:
Laser welding
Laser-additive welding
Ti_2AlNb-based alloys
Microstructure evolution
Tensile properties

ABSTRACT

The influence of the addition of filler powder on the microstructure and properties of laser-welded Ti_2AlNb joints was comparatively investigated using scanning electron microscopy, transmission electron microscopy, electron back scattered diffraction, and tensile tests. The heat affected zone (HAZ) of laser-additive-welded joints was divided into B2, B2 + α_2, and B2 + α_2 + O — three regions with increasing distance from the fusion line. The HAZ of laser-welded joints could only be divided into two regions, *viz.,* B2 + α_2 and B2 + α_2 + O. The microstructure of the fusion zone was composed of a single B2 phase for both laser welding and laser-additive welding. Columnar grains were observed in the fusion zone of laser-welded joints, while the B2 grains in the fusion zone of laser-additive-welded joints were basically equiaxed. A misorientation angle distribution analysis showed that the fraction of high-angle grain boundaries of laser-additive-welded joints was higher than that of laser-welded joints. The addition of filler powder promoted heterogeneous nucleation during solidification in laser-additive welding. Following tensile tests at room temperature, failure tended to occur in the fusion zone of the laser-welded joints and in the HAZ of the laser-additive-welded joints. The laser-additive-welded joints exhibited better tensile properties because of the higher Mo content as well as the equiaxed microstructure of the fusion zone.

1. Introduction

Ti_2AlNb-based alloys have improved oxidation and creep resistance with respect to conventional titanium aluminides. These attractive mechanical properties result from the existence of a significant volume fraction of the O (orthorhombic) phase in Ti_2AlNb-based alloys. With a stoichiometry of Ti_2AlNb, the O phase was first discovered by Banerjee et al. (1988) in a Ti-25Al-12.5Nb (at.%) alloy, and the crystal structure of the new phase was confirmed using convergent beam electron diffraction and channeling enhanced microanalysis. It was proven by Boehlert (2001) that the O phase had more active slip systems and better crack-blunting capability than the hexagonal α_2 (Ti_3Al) phase. Thus, Ti_2AlNb-based alloys have more potential than Ti_3Al-based alloys for aerospace applications. Owing to the complicated microstructure-property relationship in Ti_2AlNb-based alloys, most efforts have been directed toward optimizing the processing methods and improving the mechanical properties. Some meaningful progress was achieved in recent decades, with the research on Ti_2AlNb-based alloys gradually shifting from experimental to practical applications. Zhang et al. (2010) successfully optimized the processing methods as well as the chemical composition of a Ti-22Al-25Nb alloy, and utilized this alloy to produce structural components.

It often involves the welding technique for joining Ti_2AlNb-based alloys when coming to practical applications. The welding technique is therefore of critical importance in promoting the further applications of Ti_2AlNb-based alloys. However, compared with Ti-based alloys, the technology of manufacturing Ti-Al based intermetallics is still relatively immature, as is the welding technique. Pilot studies mainly involved fusion welding methods such as electron beam welding and laser welding. The emphasis was on the feasibility of different welding methods for joining Ti_2AlNb-based alloys. Yin et al. (2010) investigated the microstructure evolution during the electron beam welding process of a Ti-22Al-24Nb-1Mo (at.%) alloy. The fusion zone was predominantly composed of a columnar B2 phase, and no other phases were found according to the morphology analysis. Similar experimental results were obtained by Jicai et al. (2005) in the electron beam welding process of a Ti-10Al-27Nb (wt.%) alloy, indicating that the phase composition of the fusion zone remained unchanged in spite of welding parameters. However, discussions on the tensile properties of electron-beam-welded Ti_2AlNb joints were absent in the research.

* Corresponding author.
E-mail address: leizhenglong@hit.edu.cn (Z. Lei).

https://doi.org/10.1016/j.jmatprotec.2017.12.044
Received 30 August 2017; Received in revised form 28 December 2017; Accepted 30 December 2017
Available online 02 January 2018
0924-0136/

Compared to electron beam welding technology, laser welding requires no vacuum chamber and exhibits much higher welding flexibility and efficiency, which make it more suitable for joining Ti_2AlNb-based alloys in the aviation industry.

The laser weldability of a Ti-22Al-27Nb (at.%) alloy was investigated by Lei et al. (2013). Like electron-beam-welded joints, the fusion zone of laser-welded Ti-22Al-27Nb joints was also composed of columnar B2 grains. The coarse columnar B2 grains in the fusion zone resulted from the fast cooling rate in laser welding. During the fusion welding process of titanium or many other alloys, the joints often suffer a loss in tensile properties because of the columnar structure of the fusion zone. One way to improve the mechanical properties is to refine the columnar grain microstructure, because the equiaxed microstructure was believed to be more resistant to crack propagation and fracture. Yantao et al. (2014) found that the microstructure of a laser-additive-manufactured (LAM) Ti-22Al-25Nb alloy was composed of equiaxed B2 grains instead of columnar grains. In addition, the properties of the LAM Ti-22Al-25Nb alloy were comparable to those manufactured by wrought processing. This was because the filler powder could work as nuclei and promote heterogeneous nucleation during solidification.

Therefore, inspired by these facts, laser welding with filler powder, i.e, laser-additive welding, is proposed for joining Ti_2AlNb-based alloys. The laser-additive welding process is a combination of laser welding and laser-additive manufacturing. By introducing filler powder during the welding process, it is hoped that laser-additive welding will produce more equiaxed grains in the fusion zone. The coarse columnar structure in the fusion zone of laser welded joints is a common phenomenon not just in Ti_2AlNb-based alloys, but in many other alloys such as Ti-based alloys and steel. The successful application of the laser-additive welding process on Ti_2AlNb-based alloys provides a reasonable solution to improve the properties of laser welded joints of these alloys.

This work is trying to improve the microstructure in the fusion zone in order to enhance the properties of laser welded Ti_2AlNb joints. The main objective is to promote a more widespread usage of Ti_2AlNb-based alloys by proposing and developing a suitable welding technique. A second objective is to provide an insight into the microstructure-property relationship of laser-additive welded joints. In order to achieve these objectives, systematic studies were undertaken to investigate and compare the microstructural characteristics and tensile properties of the joints produced by the laser-additive welding process and conventional laser welding process.

2. Experimental

The base metal used for the welding process was 2 mm-thick Ti-22Al-24.5Nb-0.5 Mo (at.%) sheets. The chemical composition of the base metal is listed in Table 1.

Table 1
Chemical composition of Ti-22Al-24.5Nb-0.5 Mo alloy (wt.%).

Element	Mo	Al	Nb	Ti
wt. %	0.90	9.30	38.16	Balance

Table 2
Chemical composition of Ti_2AlNb powder (wt.%).

Element	Mo	Al	Nb	Ti
wt. %	3.45	9.44	39.31	Balance

The Ti_2AlNb powder used in the laser-additive welding process was manufactured using plasma-rotating-electrode process. The chemical composition of the Ti_2AlNb powder is listed in Table 2.

The base metal was cut into sections of 22.5 × 70 mm in size using wire electrical discharge machining (WEDM). In order to remove oxide layers and avoid contamination, the sections were pickled using a solution of hydrofluoric acid (HF), nitric acid (HNO_3), and distilled water before welding. After pickling, the sections were dried in an oven at 80 °C for 1 h. The laser welding process was conducted using a 3 kW CO_2 diffusion cooling laser (Rofin-Sinar DC030). Since liquid titanium reacted violently with oxygen and nitrogen, which caused a significant loss of the properties, argon was therefore adopted as both the shielding gas and back gas in laser welding and laser-additive welding. For the laser-additive welding process, the welding setup also included a coaxial cladding head (Rofin 1108-RS) and a matching powder feeder (GTV, MF-PF 2/2). At this stand-off, the focal point of the powder flow was 15 mm below that of the laser beam. Argon was also used to shield the welding process from atmospheric contamination and to deliver the powder at a steady gas flow. Fig. 1 shows a schematic of the laser welding process (Fig. 1a) and laser-additive welding process (Fig. 1b). Instead of a single pass for laser welding, three welding passes in total (one root pass and two filler passes) were required for the laser-additive welding process to construct the weld seam.

The welding parameters of laser welding and laser-additive welding are listed in Tables 3 and 4, respectively. The chemical composition of the fusion zone of the laser-additive-welded joints is shown in Table 5. The Mo content is between that of the base metal and filler powder.

The welded sections were cut transversely into metallurgical specimens by WEDM, followed by grinding, polishing, and etching. The microstructure was observed and analyzed using optical microscopy

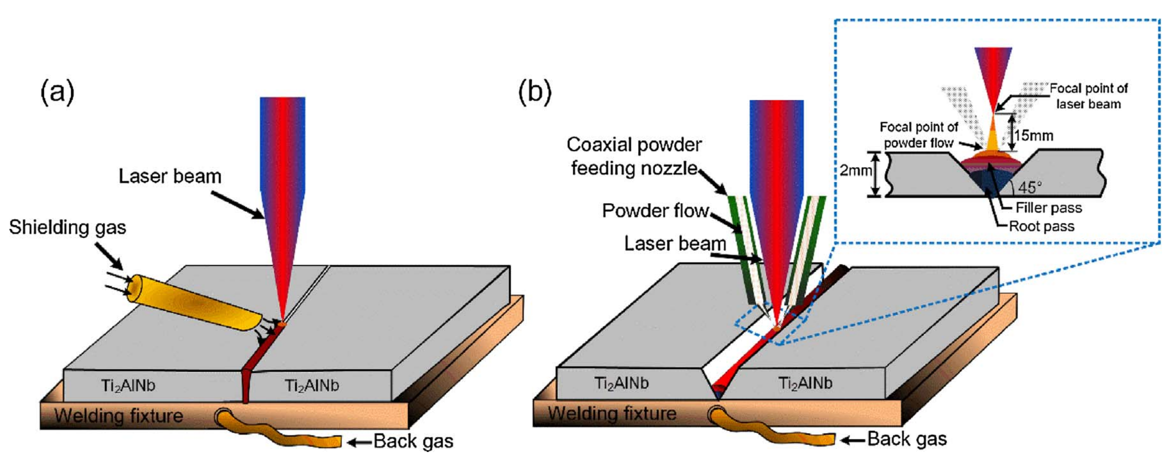

Fig. 1. Schematic diagrams of (a) laser welding and (b) laser-additive welding.